EUKARYOTIC CELL, Dec. 2011, p. 1637–1647 Vol. 10, No. 12
1535-9778/11/$12.00 doi:10.1128/EC.05182-11

Identification of Tissue Cyst Wall Components by Transcriptome Analysis of *In Vivo* and *In Vitro Toxoplasma gondii* Bradyzoites▽†

Kerry R. Buchholz,[1] Heather M. Fritz,[2] Xiucui Chen,[3] Blythe Durbin-Johnson,[3] David M. Rocke,[3] David J. Ferguson,[4] Patricia A. Conrad,[2] and John C. Boothroyd[1]*

Department of Microbiology and Immunology, Stanford University School of Medicine, Stanford, California 94305[1]; Department of Pathology, Microbiology and Immunology, School of Veterinary Medicine, University of California, Davis, California 95616[2]; Division of Biostatistics, University of California, Davis, California 95616[3]; and Nuffield Department of Clinical Laboratory Science, University of Oxford, Oxford OX3 9DU, United Kingdom[4]

Received 22 July 2011/Accepted 2 October 2011

The *Toxoplasma gondii* bradyzoite is essential to establish persistent infection, yet little is known about what factors this developmental form secretes to establish the cyst or interact with its host cell. To identify candidate bradyzoite-secreted effectors, the transcriptomes of *in vitro* tachyzoites 2 days postinfection, *in vitro* bradyzoites 4 days postinfection, and *in vivo* bradyzoites 21 days postinfection were interrogated by microarray, and the program SignalP was used to identify signal peptides indicating secretion. One hundred two putative bradyzoite-secreted effectors were identified by this approach. Two candidates, bradyzoite pseudokinase 1 and microneme adhesive repeat domain-containing protein 4, were chosen for further investigation and confirmed to be induced and secreted by bradyzoites *in vitro* and *in vivo*. Thus, we report the first analysis of the transcriptomes of *in vitro* and *in vivo* bradyzoites and identify two new protein components of the *Toxoplasma* tissue cyst wall.

Asexual replication of the protozoan parasite *Toxoplasma gondii* occurs through two developmental forms, the rapidly growing tachyzoite and the bradyzoite, which is slow growing and forms tissue cysts. Tachyzoites replicate during acute infection, but after about a week, conversion to bradyzoites occurs (31). This switch to the bradyzoite form is vital to the parasite's life cycle and allows the persistent infection of intermediate hosts until they are ingested by the feline definitive host, where the sexual cycle takes place. Infection in an immunocompetent human is controlled, but the parasite is not eradicated; instead, it persists in a bradyzoite form in brain and muscle tissues (34). While this initial infection is commonly asymptomatic, reactivation of tissue cysts when the immune system is suppressed can cause life-threatening encephalitis and other clinical manifestations (34). How *Toxoplasma* bradyzoites are able to evade the immune system, maintain cysts, and persist in the host for decades after the initial infection is not understood.

Toxoplasma is an obligate intracellular pathogen, and both bradyzoites and tachyzoites reside in a parasitophorous vacuole (PV) that appears to be necessary for intracellular growth. The parasite secretes proteins into the PV, onto the PV membrane, and into the host cell cytosol through its secretory organelles, i.e., the rhoptries and dense granules (9, 10). While there is much research elucidating how proteins secreted by the tachyzoite form of *Toxoplasma* function to modify its intracellular environment, little is known about how bradyzoites interact with the host or how cysts are established and maintained. This is especially true for the cyst wall itself, where relatively few proteins have been identified (15, 49). Initial studies to identify bradyzoite-secreted proteins performed by Schwarz et al. used expressed sequence tag data for only 5% of the genome and identified bradyzoite rhoptry protein 1 (BRP1) (45). The discovery of a bradyzoite secreted protein by the screening of such a small percentage of the genome suggested that numerous other such proteins may exist.

Differentiation of *Toxoplasma* from the tachyzoite to the bradyzoite form results in significant changes in the parasite and PV (17). Bradyzoites express specific surface antigens (e.g., SAG1-related sequence 9, SAG2X) and metabolic factors (e.g., lactate dehydrogenase 2 [LDH2], enolase 1 [ENO1]) while downregulating others found in tachyzoites (e.g., SAG1, LDH1, ENO2) (31). The study of bradyzoites and tissues cysts has been facilitated by the *in vitro* model of differentiation whereby *Toxoplasma* tachyzoites are induced to form bradyzoites through various stress-inducing treatments, including low serum, alkaline pH, and gamma interferon (48). *In vivo*- and *in vitro*-derived cysts are similar in their expression of certain key antigens and in being contained within a cyst wall that is detectable by staining with the lectin *Dolichos biflorus* agglutinin (DBA) and that appears ultrastructurally similar *in vitro* and *in vivo* by transmission electron microscopy. In other respects, however, *in vitro* cysts differ from those found *in vivo* in terms of size, the number of bradyzoites within the cyst, and longevity (17). This raises the question of how accurately the *in vitro* culture system of bradyzoites models *in vivo* bradyzoites. The transcriptomes of *in vitro* bradyzoites and tachyzoites have been interrogated with a variety of strains and conditions (13, 30, 38; unpublished data from various groups available at ToxoDB.org). The difficulty involved in obtaining enough par-

* Corresponding author. Mailing address: Fairchild Science Building, Room D305, 299 Campus Drive, Stanford University School of Medicine, Stanford, CA 94305-5124. Phone: (650) 723-7984. Fax: (650) 725-6757. E-mail: john.boothroyd@stanford.edu.

† Supplemental material for this article may be found at http://ec.asm.org/.

▽ Published ahead of print on 21 October 2011.

asite material from *in vivo* sources, however, has previously precluded transcriptomic investigations of *in vivo* bradyzoites.

The goals of this study were to characterize bradyzoite gene expression and use these data to better understand bradyzoite development, especially proteins secreted by bradyzoites but not tachyzoites. To accomplish this, we used *T. gondii* M4 to isolate *in vivo* cysts and used these to compare the transcriptomes of *in vivo* bradyzoites, *in vitro* bradyzoites, and *in vitro* tachyzoites. Two novel candidates identified with these data were endogenously epitope tagged and confirmed as bradyzoite-secreted proteins that localize to the cyst matrix and cyst wall.

MATERIALS AND METHODS

Cell culture and parasite strains. Parasites were cultured in confluent primary human foreskin fibroblasts (HFFs) grown in Dulbecco's modified Eagle's medium (DMEM; Invitrogen, Carlsbad, CA) with 10% fetal calf serum (FCS; HyClone, Logan, UT), 2 mM glutamine, 100 U/ml penicillin, and 100 μg/ml streptomycin (complete DMEM [cDMEM]) at 37°C with 5% CO_2.

The M4 parasite strain used for all of the microarray analyses in this study was a gift from Lee Innes at the Moredun Research Institute, Edinburgh, Scotland (25). Based on sequencing at four polymorphic loci (SAG3, B1, GRA2, and toxofilin; data not shown), all of which yielded a sequence identical to that of the canonical type II strain ME49 (ToxoDB.org), this is presumed to be a type II strain. The parental strain used in this study for protein tagging and localization was the type II Prugniaud (Pru) strain lacking a functional hypoxanthine-xanthine-guanine-phosphoribosyltransferase gene (*HXGPRT*) which was a gift from D. Soldati (University of Geneva, Geneva, Switzerland).

***In vitro* differentiation and culture of bradyzoites.** Differentiation to the bradyzoite form was induced by growth under alkaline conditions essentially as described previously (23). Briefly, confluent monolayers of HFFs were infected with tachyzoites at a multiplicity of infection of 3 for 4 h in cDMEM at 37°C with 5% CO_2. The cells were washed twice with phosphate-buffered saline (PBS) and cultured in RPMI medium (Invitrogen) lacking sodium bicarbonate with 1% FCS, 10 mg/ml HEPES, 100 U/ml penicillin, and 100 μg/ml streptomycin, pH 8.0, and grown at 37°C without supplemented CO_2 to induce differentiation to the bradyzoite form.

Isolation of *in vitro* bradyzoites and tachyzoites. *In vitro* bradyzoites were prepared at 4 or 8 days postinfection (dpi), and *in vitro* tachyzoite samples were obtained at 2 dpi. Duplicate cultures were infected, harvested, and processed independently. To isolate the parasites, HFFs were lysed by passage through a 27-gauge needle at least 10 times. To minimize host cell contamination, unlysed cells were pelleted by brief centrifugation (~3 min) in a Sorvall RT7 plus tabletop centrifuge at 700 rpm (102 × *g*). The supernatant was removed, and parasites were collected by centrifugation at 1,500 rpm (470 × *g*) for 10 min, resuspended in TRIzol reagent (Invitrogen), and frozen at −80°C.

Isolation of *in vivo* bradyzoites. (i) Bradyzoite cyst production. *In vivo* bradyzoites were produced and isolated as described by Fritz et al. (22a). Two groups of four 8-week-old Swiss Webster mice were infected with 1,000 oocysts perorally. One of these mice was subcutaneously inoculated with 1,000 oocysts. The mice were treated with 0.44 μg/ml sulfadiazine in their water 11 to 21 dpi. Three weeks after inoculation, the mice exhibited neurological impairment and were sacrificed and the brains were harvested. One-quarter of each mouse brain was reserved for histopathology. The remaining three-quarters of each brain was processed for bradyzoite cyst isolation. All animal experiments were conducted with the approval and oversight of the Institutional Animal Care and Use Committee at the University of California Davis or Stanford University.

(ii) Bradyzoite cyst isolation. The method used to harvest bradyzoite cysts from mouse brains was modified and optimized from a previously described protocol (28). Each brain was passed through a 100-μm cell strainer, washed once, and resuspended in PBS to a total volume of 4 ml. The brain suspension was then passed 10 times through 16- and 22-gauge blunt needles and brought to a total volume of 10 ml with PBS. A density gradient was prepared for each sample by layering (from bottom to top) 9 ml 90% (vol/vol) Percoll in PBS (GE Healthcare, Piscataway, NJ), 9 ml 30% Percoll, and 10 ml brain suspension in a 50-ml conical tube. Each gradient was centrifuged at 1,200 × *g* for 15 min at 4°C. The cysts were harvested from the 30% portion and the 30%/90% interface. This was done by first removing and discarding the top 10 ml. Then 14 ml was removed to a fresh tube, which contained the desired cyst-containing fraction. The pellet was also discarded. The cyst suspensions were washed with PBS by bringing the volume to 45 ml with PBS and centrifuging it at 1,500 × *g* for 15 min at 4°C. The supernatant was removed to about 5 ml, and the pellets were combined into one 50-ml tube. A second wash in PBS was performed by bringing the combined suspension to 45 ml with PBS and centrifuging it at 2,500 × *g* for 15 min at 4°C. The supernatant was removed, and the remaining pellet was transferred to a 1.5-ml microcentrifuge tube and brought to 1 ml with PBS. A 10-μl volume was removed to count cysts. We obtained 56,400 pooled purified cysts from group A (4 mice) and 48,900 cysts from group B (4 mice). The resulting suspension was then centrifuged at 13,200 rpm for 8 min, and the supernatant was removed. The final cyst pellet was resuspended in 1 ml TRIzol reagent and stored in siliconized tubes (Axygen Maxymum Recovery; Axygen Inc., Union City, CA) at −80°C until RNA was extracted.

RNA isolation, labeling, and microarray hybridization. Total RNA was purified using TRIzol reagent according to the manufacturer's protocol, resuspended in water, and stored in siliconized tubes at −80°C. The 3′ IVT express kit (Affymetrix, Santa Clara, CA) was used to label 250 ng of total RNA in accordance with the manufacturer's protocol. Samples (7.5 μg) of labeled, fragmented, amplified RNA were hybridized on the Tgondiia520372 custom chip by Affymetrix (3) at the Stanford Protein and Nucleic Acid Facility using Affymetrix GeneChip Hybridization Oven 640, Affymetrix GeneChip Fluidics Station 450, and Affymetrix GeneChip Scanner 3000 7G. The software used was Affymetrix GeneChip Command Console.

Preprocessing. Data were converted from .cel files and averaged across probes within each probe set using the Bioconductor package affy (version 1.22.1 [24]) within the statistical software system R (version 2.10.1 [40]) and then transformed via a generalized logarithm (glog) transformation (18, 27) using the Bioconductor package LMGene (version 2.4.0 [42]).

Statistical analysis. A one-way analysis-of-variance (ANOVA) model was fitted to the data one probe set at a time. For probe sets for which the global F test was significant at the 5% level, indicating significant differences between at least two levels of the factor, Tukey honestly significant difference (HSD) *post hoc* tests were conducted to test for significant differences among the comparisons of interest.

Generation of endogenously tagged bradyzoites. All of the primers used for these studies can be found in Table S1 in the supplemental material. Targeting plasmids were engineered to generate *Toxoplasma* strains where the endogenous *BPK1* or *MCP4* locus was replaced with one fused to a C-terminal hemagglutinin (HA) tag using the pTKO vector (37). Briefly, ~1- to 2-kb regions immediately up- or downstream of the targeted gene's stop codon were inserted flanking a cassette for expression of the selectable marker *HXGPRT*. The HA tag sequence was added to the reverse primers so as to be incorporated into the 5′ targeting sequence during amplification. The 5′ targeting sequence upstream of the stop codon does not contain the promoter or start codon of the targeted gene to avoid ectopic expression from the vector. Targeting plasmids were linearized by digestion with the enzyme NotI. The plasmid (15 to 30 μg) was transfected into *T. gondii* PRUΔ*hxgprt* by electroporation as previously described by Soldati and Boothroyd (46). Mycophenolic acid (50 μg/ml) and xanthine (50 μg/ml) were used to select for stable integration as previously described (16), and single clones were isolated by limiting dilution. To confirm a double recombination event, selected clones were screened for the absence of expression of red fluorescent protein (mCherry), as the mCherry gene is positioned upstream of the 5′ targeting sequence in the constructed vector. To confirm correct integration of the vector into the genome, genomic DNA was screened by PCR using primers within the vector and in the genomic sequence (outside the region used for targeting; see Table S1 in the supplemental material) and confirmed by sequencing.

Immunoblot assay. Parasites were lysed from HFFs by multiple passages through a 27-gauge needle. Equal numbers of parasites were resuspended in SDS-PAGE loading buffer, boiled for 10 min, and frozen at −20°C. We loaded 5×10^5 parasite equivalents per sample and subjected the samples to 10% SDS-PAGE. Immunoblot analysis was performed using standard methods. Monoclonal antibody 3F10 (a rat anti-HA antibody) conjugated to horseradish peroxidase (HRP; Roche) was used to probe the membrane. The membrane was stripped and probed with rabbit anti-SAG2X (43) in 5% bovine serum albumin (BSA). The membrane was again stripped and reprobed with rabbit anti-SAG1. All incubations were conducted with 10 mM Tris–150 mM NaCl, pH 7.4 (TBS), supplemented with 5% milk and 0.05% Tween 20, unless otherwise noted, and followed by exposure to an appropriate secondary antibody conjugated to HRP.

Immunofluorescence assays (IFAs). For *in vitro* localization, *Toxoplasma*-infected HFF cells on glass coverslips were fixed with 3.5% formaldehyde for 20 min. All subsequent incubations were performed in PBS supplemented with 3% BSA. Cells were blocked in 3% BSA in PBS overnight at 4°C or at room

temperature for 1 h and then permeabilized for 20 to 60 min with PBS supplemented with 0.3 to 0.5% Triton X-100. Proteins with the HA epitope were detected using the monoclonal antibody 3F10, followed by goat anti-rat 594 Alexa Fluor-conjugated secondary antibodies (Molecular Probes). DBA (Vector Laboratories, Burlingame, CA) was used as a marker of the cyst wall. Samples were viewed on an Olympus BX60 upright fluorescence microscope with a 100× oil immersion lens, and images were acquired with Image-Pro Plus software. Images were minimally and equally adjusted within groups using Adobe Photoshop CS3.

For *in vivo* localization, female CBA/J mice were infected intraperitoneally with 5,000 parasites. At 40 dpi, the mice, prior to sacrifice, were anesthetized with a mixture of ketamine (24 mg/ml) and xylazine (48 mg/ml) according to weight. Prior to intracardiac perfusion with heparin (10 U/ml) in a 0.9% saline solution, the mice were confirmed to be unresponsive to deep pain stimulation. The brain was drop fixed in 4% paraformaldehyde in phosphate buffer (pH 7.4) overnight at 4°C and imbedded in 30% sucrose in PBS until sectioned. Prior to sectioning, the brain was frozen in isopentane on dry ice and sectioned into 40-μm coronal sections using a rotary cryotome. Sections were washed in TBS 3 times for 5 min and blocked and permeabilized in 3% BSA in TBS plus 0.3% Triton X-100 for 1 h. Sections were incubated overnight at 4°C in 1% BSA plus 0.3% Triton X-100 along with 3F10 rat anti-HA (Roche) and DBA conjugated to rhodamine. Sections were washed as before and incubated for 4 h 30 min at room temperature in PBS supplemented with 1% BSA and 0.3% Triton X-100 along with goat anti-rat 488 (Alexa Fluor-conjugated secondary antibodies; Molecular Probes) and DBA conjugated to rhodamine. Sections were washed, mounted on glass slides, and viewed with a Plan-Apo 100× oil objective lens on a Zeiss LSM 510 confocal laser scanning microscope at the Cell Science Imaging Facility of Stanford University. These experiments were conducted with the approval and oversight of the Institutional Animal Care and Use Committee at Stanford University.

Immunoelectron microscopy (EM). *In vitro* (5 dpi) and *in vivo* (isolated from mouse brain) tissue cysts were collected and fixed in 2% paraformaldehyde in 0.1 M phosphate buffer. Mouse brains were obtained 40 dpi as described above. *In vivo* cysts were isolated by passage over Percoll (GE Healthcare) gradients as described above but without passage through 16- and 22-gauge needles, and the final cyst pellet was brought up in 2% paraformaldehyde in 0.1 M phosphate buffer, pH 7.2. Samples were then dehydrated and embedded in LR White resin. Thin sections were collected on Formvar-coated grids and floated on drops of 1% BSA in PBS buffer to block the background and then on drops of rabbit anti-HA (Invitrogen) in PBS buffer. After being washed, the sections were floated on drops of goat anti-rabbit Ig conjugated to 10-nm colloidal gold (British Biocell International Ltd.), washed, and stained with uranyl acetate prior to examination in the electron microscope.

Microarray data accession number. The complete data set obtained in this study has been deposited in the Gene Expression Omnibus database (GSE32427) and has also been provided to ToxoDB.org, where it is accessible in a searchable format.

RESULTS

Isolation of *T. gondii* tachyzoites and bradyzoite. The difficulty in obtaining sufficient quantities of parasite RNA without overwhelming contamination with host material has previously precluded transcriptome analysis of *in vivo* bradyzoites. To circumvent this problem, we used strain M4, which has been maintained by passing from cat to mouse to cat, initiated the mouse infections with oocysts, and used sulfadiazine treatment from 11 to 21 dpi to prevent death of the animals during the acute phase of infection (22a). This protocol enabled us to obtain a high number of *in vivo* bradyzoite cysts. We obtained 56,400 pooled purified cysts from the four mice in group A and 48,900 cysts from the four in group B.

To obtain *in vitro* tachyzoites and bradyzoites, *T. gondii* M4 was minimally passed in HFF cells. Tachyzoites were harvested at 2 dpi, at which time parasite vacuoles were full but the parasites had not yet exited from the host cell. Bradyzoites were harvested after 4 days of growth in differentiation medium, at which time the cyst wall typically has formed (as detected by DBA staining) and parasites express bradyzoite-specific antigens (SAG2X), as well as after 8 days of growth in such medium. These methods do not yield 100% pure tachyzoite or bradyzoite cultures, and so, to estimate their relative purity, parallel infections on glass coverslips were fixed at the time of RNA harvesting and stained for the tachyzoite surface antigen SAG1 and the bradyzoite surface antigen SAG2X. The $SAG1^+$ and/or $SAG2X^+$ parasite vacuoles were then enumerated. In 2-dpi tachyzoite cultures, 8% of the vacuoles were found to contain parasites displaying a bradyzoite pattern ($SAG2X^+$ $SAG1^-$), with that number rising to 14% if double-staining ($SAG2X^+$ $SAG1^+$) vacuoles were included as "bradyzoite" (data not shown). Less than 5% of the vacuoles in 4-dpi bradyzoite cultures were "tachyzoite" ($SAG2X^-$ $SAG1^+$), with that number rising to 8% if double-staining ($SAG2X^+$ $SAG1^+$) vacuoles were included.

***T. gondii* M4 microarrays.** To analyze the transcriptome of the *Toxoplasma* tachyzoite and bradyzoite samples, whole-genome expression profiling was performed using the Affymetrix ToxoGeneChip microarray (3). This array interrogates 8,058 predicted *Toxoplasma* genes (version 4.0 genome annotation) using 3′-biased probes (3). The data obtained from these arrays were transformed by the glog transformation (18) and normalized with the LOWESS algorithm using the Bioconductor package LMGene (version 2.4.0 [42]) as described in Materials and Methods.

To determine how analogous the 2-dpi *in vitro* tachyzoite (2d Tachy), 4-dpi *in vitro* bradyzoite (4d Brady), 8-dpi *in vitro* bradyzoite (8d Brady), and 21-dpi *in vivo* bradyzoite (21d Brady) data sets were, the mean expression values for each probe set were plotted and the correlation coefficient (R^2) was calculated for each pairwise comparison. As expected, the 21d Brady *in vivo* samples showed a higher correlation with the *in vitro* bradyzoite sample (4d Brady; Fig. 1A) than with tachyzoites (2d Tachy; Fig. 1B), while the 2d Tachy samples showed a higher correlation with the sample of younger bradyzoites formed *in vitro* (4d Brady; Fig. 1C) than the *in vivo* material (Fig. 1B). The 8d Brady *in vitro* samples were not more highly correlated than the 4d Brady samples are to the 21d Brady *in vivo* samples but were slightly less similar (8d Brady versus 21d Brady, R^2 of 0.815; data not shown). The 4d Brady and 8d Brady expression data were very highly correlated, with an R^2 value of 0.935 (data not shown). To facilitate discussion of the data, therefore, this paper will focus on the 4d Brady data; 8d Brady data can be found in Table S2 in the supplemental material.

To determine what pairwise differences in expression were significant, a one-way ANOVA and a Tukey HSD *post hoc* test were applied to the data. The complete set of significantly changed probe sets for any comparison is shown in Table S2 in the supplemental material. The microarray used is based on the version 4.0 *T. gondii* genome annotation, and therefore not all probe sets have a corresponding gene ID in the current version 5.0 annotation and not all currently annotated genes have a corresponding probe set. A summary of the array results is shown in Table 1. Five hundred fifty probe sets were significantly changed between 2d Tachy and 4d Brady, with 60% (332) increasing and 40% (218) decreasing (Table 1). The number of significant changes increased to 831 when the 21d Brady data were compared to the 2d Tachy data, with 57% (470) of the probe sets increased in the 21d Brady data and

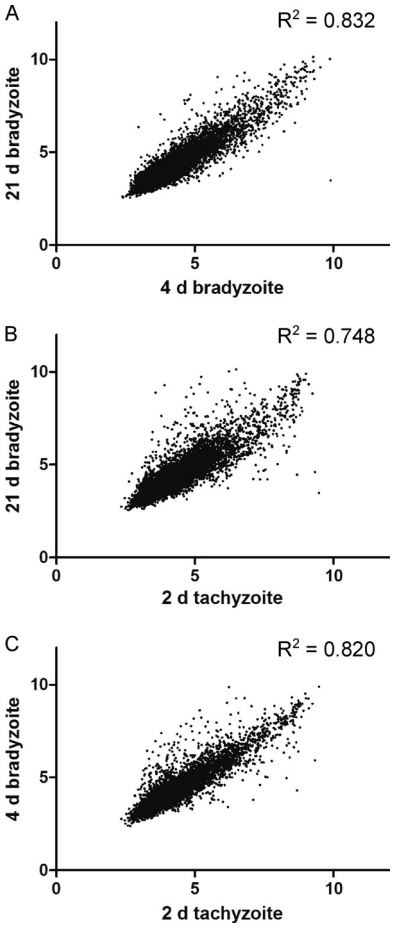

FIG. 1. Scatterplots of average normalized expression values. Probe sets to *Toxoplasma* genes were normalized as described in Materials and Methods, average values for replicate arrays were plotted, and the correlation coefficient (R^2) was determined using Prism software. Samples corresponded to tachyzoites grown for 2 days on HFF cells (2d Tachy), bradyzoites that had been grown on HFFs for 4 days *in vitro* (4d Brady), and tissue cysts harvested from infected mouse brains 21 days after oral infection with oocysts (21d Brady). The comparisons are 21d Brady versus 4d Brady (A), 21d Brady versus 2d Tachy (B), and 4d Brady versus 2d Tachy (C).

43% (361) decreased (Table 1). As expected, the number of significantly changed genes reflected the correlation (R^2) data; i.e., the comparisons of less correlated data resulted in a higher number of significantly changed probe sets.

To confirm the validity of the various data sets, the expression of known developmentally regulated genes was assessed. The array expression values of bradyzoite-specific bradyzoite antigen 1 (*BAG1*), *ENO1*, bradyzoite rhoptry protein 1 (*BRP1*), *LDH2*, and *SRS9* were all significantly higher in the two bradyzoite samples than in the tachyzoite samples (Table 2) (29, 31, 45), while those of the well-studied, tachyzoite-specific proteins, including ENO2, LDH1, SAG1, SAG2A, and SRS2, were all substantially lower (Table 2) (31). These results confirmed that, as expected, the microarray approach used here yields an accurate portrayal of differences in gene expression during asexual development in *Toxoplasma*.

Changes in transcript profiles between tachyzoite-to-bradyzoite developmental forms and between *in vitro* and *in vivo* bradyzoites. As expected, many of the genes/probe sets that showed a difference in expression between the *in vitro* 4d Brady and 2d Tachy samples were similarly higher or lower in the *in vivo* 21d Brady samples. Numerous differences, however, were also found between the *in vitro* and *in vivo* bradyzoite parasites: Five hundred ninety-five probe sets were significantly changed in 21d Brady versus 4d Brady samples. These can be grouped into three categories of regulation based on how they change during development. First are those that are changed only in the *in vivo* bradyzoites (267, 45%). This includes transcripts for the putative rhoptry kinase ROP28 and MIC12, which were both upregulated in the 21d Brady versus the 4d Brady and 2d Tachy samples (see Table S3A and B in the supplemental material). Second are changes where levels significantly change in 4d Brady versus 2d Tachy samples but then return to tachyzoite levels in the 21d Brady samples (112, 19%). Genes in this category include several SAG/SRS genes (e.g., SAG5A and SRS13; see Table S5 in the supplemental material), MIC10, and GRA7 (see Table S3A and C in the supplemental material). Third are probe sets/genes that are significantly up- or downregulated in a progressive fashion, further increasing or decreasing in transcript levels from 2d Tachy to 4d Brady to 21d Brady samples (34, 6%). These include canonical developmentally regulated genes such as *LDH2* and *SAG2Y* (Table 2). Thus, while many genes are similarly regulated between the *in vitro* and *in vivo* bradyzoites, these data also show regulation of transcript levels as bradyzoite development progresses.

Proteins secreted by *Toxoplasma* from its secretory organelles, the micronemes, rhoptries, and dense granules, are important for attachment, invasion, establishment of the PV, and interaction with the infected cell (9, 10). This is true of both tachyzoites and bradyzoites, but these two developmental

TABLE 1. Summary of array results comparing *Toxoplasma* tachyzoites and bradyzoites produced *in vitro* and bradyzoites formed *in vivo* in the brains of experimentally infected mice

Comparison	Total no. of significantly changed probe sets	No. (%) increased	No. (%) decreased	No. also significantly changed[a] in:			
				4dB vs 2dT	8dB vs 2dT	21dB vs 2dT	21dB vs 4dB
4-day *in vitro* bradyzoites vs 2-day tachyzoites	550	332 (60)	218 (40)		353	311	166
8-day *in vitro* bradyzoites vs 2-day tachyzoites	533	379 (71)	153 (29)	353		283	146
21-day *in vivo* bradyzoites vs 2-day tachyzoites	831	470 (57)	361 (43)	311	283		321
21-day *in vivo* bradyzoites vs 4-day *in vitro* bradyzoites	595	339 (57)	256 (43)	166	146	321	

[a] 4dB, 4-dpi bradyzoites; 8dB, 8-dpi bradyzoites; 21dB, 21-dpi bradyzoites; 2dB, 2-dpi tachyzoites.

TABLE 2. Known bradyzoite and tachyzoite developmentally regulated genes

Probe set	Gene ID	Gene name	Product	Avg expression[a]				Fold change[b]			
				2dT	4dB	8dB	21dB	4dB vs 2dT	8dB vs 2dT	21dB vs 2dT	21dB vs 4dB
Upregulated in bradyzoites versus tachyzoites											
55.m00009_at	TGME49_059020	*BAG1*	Heat shock protein, bradyzoite antigen	6.2	9.9	9.4	10.0	29	18	34	—
59.m03411_at	TGME49_068860	*ENO1*	Enolase 1	5.2	8.6	8.5	9.3	18	16	36	2.0
583.m09133_at	TGME49_114250	*BRP1*	Bradyzoite rhoptry protein	5.0	8.2	7.6	8.8	13	7.2	23	—
23.m00149_s_at	TGME49_007130	*SAG2Y*	Surface antigen (SRS49A)	4.8	6.2	6.0	7.2	2.3	2.0	5.4	2.3
641.m01562_at	TGME49_120190	*SRS9*	Surface antigen (SRS16B)	4.1	5.5	5.6	5.6	2.0	2.0	2.1	—
80.m00010_at	TGME49_091040	*LDH2*	Lactate dehydrogenase 2	4.9	7.8	7.7	9.2	9.1	8.5	34	3.8
Downregulated in bradyzoites versus tachyzoites											
59.m03410_at	TGME49_068850	*ENO2*	Enolase 2	7.3	4.6	5.3	4.2	0.15	0.21	0.13	—
59.m00008_at	TGME49_071050	*SAG2A*	Surface antigen (SRS34A, P22)	8.4	6.9	7.2	6.0	0.24	—	0.12	—
44.m00010_at	TGME49_033480	*SRS2*	Surface antigen (SRS29C, P35)	7.6	5.0	5.3	4.2	0.14	0.16	0.10	—
44.m00009_at	TGME49_033460	*SAG1*	Surface antigen (SRS29B, P30)	9.3	5.9	7.1	4.6	0.05	0.12	0.02	—
44.m00006_at	TGME49_032350	*LDH1*	Lactate dehydrogenase 1	6.0	5.4	5.5	5.1	—	—	0.55	—

[a] 4dB, 4-dpi bradyzoites; 8dB, 8-dpi bradyzoites; 21dB, 21-dpi bradyzoites; 2dB, 2-dpi tachyzoites. Average normalized glog-transformed expression values.
[b] Fold change calculated from glog mean expression values back-transformed to the original scale (see Materials and Methods) and shown only where values are significantly different ($P < 0.05$). —, fold change not significant.

forms differ in the cells they tend to infect and in their respective roles in the parasite's life cycle. Given these major differences in the niches occupied by tachyzoites and bradyzoites, as well as apparent differences in their metabolism (31), we investigated overall changes in genes grouped by function (see Tables S3 to S5 in the supplemental material). Significant changes in the transcript levels for microneme-, rhoptry-, and dense-granule-localized proteins were seen (see Table S3 in the supplemental material), suggesting possible differences between tachyzoites and bradyzoites in attachment, invasion, and PV function. Twenty-two metabolism-related genes were also differentially regulated between the two developmental forms, including the well-described *LDH1*/2 and *ENO1*/2 genes (Table 2; see Table S4 in the supplemental material). This is consistent with previous data describing differential sugar metabolism between tachyzoites and bradyzoites (2, 14). As expected, surface antigens (SAG domain containing) made up one of the largest groups of developmentally regulated genes (see Table S5 in the supplemental material), with 33 significantly different in one or more of the pairwise comparisons. Of note is the uncharacterized putative surface antigen SRS22A, which is encoded by the most highly upregulated SAG-related gene in 21d Brady versus 2d Tachy (55.6-fold) samples and 21d Brady versus 4d Brady (10.5-fold) samples.

Identification of putative bradyzoite secreted proteins. Due to their likely importance to the parasite's biology, we chose to focus our attention on novel secreted proteins that the microarray data predict are upregulated in bradyzoites. For this, we used the program SignalP 3.0 to identify proteins that contain a predicted signal peptide for entry into the secretory pathway (7, 35, 36). Although this program has been previously shown to be generally accurate in predicting secreted proteins in *Toxoplasma* (19, 45), it is likely that there will be some miscalls both positively and negatively. Likewise, we are dependent on the accuracy of the gene prediction algorithms used within ToxoDB in predicting the true N terminus of a protein. This is key for identifying signal peptides but is one of the most difficult challenges for such software. Nevertheless, we felt it important to explore this crucial class of proteins.

To focus our efforts on proteins that are likely to play novel roles, SAG-related proteins were eliminated from further investigation as these have been well studied for their roles in invasion and immune evasion but are not believed to enter the host cell or directly modulate host function (29, 43). Candidates which have been previously identified and investigated are noted (superscript letter b in Table S6 in the supplemental material) and were not considered for further inquiry in this study. A total of 102 candidates that satisfy these criteria were identified in this screen. These include 2 MIC homologues, 4 which contain plasminogen apple nematode (PAN) domains, 3 putative oocyst wall components, and 4 with predicted kinase domains (see Table S6 in the supplemental material).

Endogenous tagging of secreted bradyzoite proteins. To further investigate and confirm the secretion of the bradyzoite-upregulated proteins identified in our SignalP analysis, two candidates were chosen based on their homology to functional domains in known secreted proteins demonstrated to be important for *Toxoplasma* survival (11, 22, 41) (Table 3). The first, TGME49_053330/52.m01578, contains sequence homology to the catalytic domain of protein kinases; however, as it lacks residues that are known to be important for catalytic activity (26), this protein is likely a pseudokinase (see Fig. S1 in the supplemental material). Therefore, we have named this protein bradyzoite pseudokinase 1 (BPK1). The second protein, TGME49_008730/25.m01822, also known as MAR (mi-

TABLE 3. Candidate bradyzoite-secreted factors chosen for further investigation

Probe set	Gene ID	Gene name	Description	Avg expression[a]			Fold change[b]		
				2dT	4dB	21dB	4dB vs 2dT	21dB vs 2dT	21dB vs 4dB
52.m01578_at	TGME49_053330	*BPK1*	Kinase domain	5.8	8.0	8.3	6.3	8.4	—
25.m01822_at	TGME49_008730	*MCP4*	MAR domain	5.1	6.6	6.6	2.8	2.7	—

[a] 4dB, 4-dpi bradyzoites; 21dB, 21-dpi bradyzoites; 2dB, 2-dpi tachyzoites. Average normalized glog-transformed expression values.
[b] Fold change calculated from glog mean expression values back-transformed to the original scale (see Materials and Methods) and shown only where values are significantly different ($P < 0.05$). —, fold change not significant.

croneme adhesive repeat) domain-containing protein 4 (MCP4), was recently described by Friedrich et al. as part of a MAR domain-containing family of proteins in *Toxoplasma* and *Neospora* (22).

To examine the protein levels and localization of BPK1 and MCP4 in the different developmental stages, an HA tag was independently introduced into the C termini of both proteins for the purpose of immunoblotting and IFA. The coding sequence of the HA tag was introduced into the endogenous locus to maintain the native promoters and thus the normal levels and timing of expression. Parasites expressing HA-tagged derivatives of BPK1 or MCP4 were generated in PRUΔ*hxgprt* using a vector to homologously recombine the *HXGPRT* gene flanked by targeting sequences upstream and downstream of the 3′ end of the *BPK1* or *MCP4* gene (37). Following selection for the *HXGPRT* marker in medium supplemented with mycophenolic acid/xanthine, individual clones were confirmed by PCR and sequencing of the genomic DNA (data not shown).

To determine if the protein levels reflect the transcript data obtained for BPK1 and MCP4, total lysates obtained from equal numbers of 2-dpi tachyzoites, 2-dpi bradyzoites, and 4-dpi bradyzoites expressing either BPK1-HA or MCP4-HA or the parental control strain PRUΔ*hxgprt* were analyzed by immunoblotting using antisera for the HA tag, as well as for control antigens, to confirm a switch between the developmental forms under these conditions (Fig. 2). Immunoblotting for the tachyzoite antigen SAG1 demonstrated that the levels of this protein were, as expected, reduced in the 2- and 4-dpi bradyzoites, relative to those in the 2-dpi tachyzoites (Fig. 2). Furthermore, immunoblotting for the bradyzoite surface antigen SAG2X demonstrated that this protein could be detected, as expected, in 4-dpi bradyzoites, while it could not be detected in the 2-dpi tachyzoites (Fig. 2). In those parasites expressing BPK1-HA, we observed that there was an apparent increase in the levels of this protein in the 2- and 4-dpi bradyzoites versus the 2-dpi tachyzoites, as determined by immunoblotting with the HA-specific antisera (Fig. 2, lanes 5 to 7). While this increase in the levels of BPK1-HA protein in bradyzoites versus those in tachyzoites is consistent with the transcript data on BPK1, we also observed that significant levels of BPK1-HA could be detected in the 2-dpi tachyzoites sample (Fig. 2, lane 5). In parasites expressing MCP4-HA, we observed that this protein could be detected in 4-dpi bradyzoites (Fig. 2, lane 10). Unlike the immunoblotting results for BPK1-HA, however, MCP4-HA was not detected in 2-dpi tachyzoites or 2-dpi bradyzoites (Fig. 2, lanes 8 and 9). Collectively, these results demonstrate that BPK1 and MCP4 protein levels increase during tachyzoite-to-bradyzoite conversion in a manner that is consistent with the increase in their transcript levels as detected by microarray analyses.

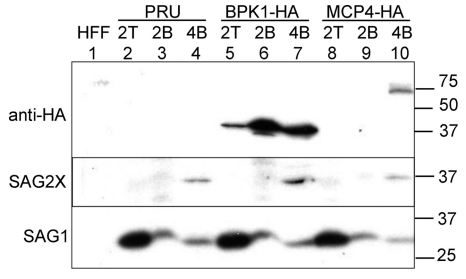

FIG. 2. BPK1 and MCP4 are induced by bradyzoites. HFF monolayers were infected with the PRUΔ*hxgprt* strain of parasites that had been engineered to express a BPK1 or MCP4 protein fused to a C-terminal HA tag (BPK-HA and MCP4-HA, respectively) for 2 days under tachyzoite and 2 days and 4 days under bradyzoite growth conditions. Parasites were released from cells by syringe lysis and counted before SDS-PAGE loading buffer was added. A total of 5×10^5 parasite equivalents were added per lane and probed with antibodies specific for HA, SAG1, or SAG2X as described in Materials and Methods. Representative images from at least two independent experiments are shown. The values to the right are molecular sizes in kilodaltons.

BPK1 and MCP4 localization *in vitro*. In addition to being developmentally regulated, BPK1 and MCP4 were selected for further characterization based on the prediction that they may be secreted proteins. To verify that these proteins are secreted by bradyzoites and to determine where they localize during infection, HFF monolayers were infected under tachyzoite and bradyzoite conditions with the BPK1-HA- or MCP4-HA-expressing parasites, and the infected monolayers were examined by IFA using an HA-specific antibody. Confirming the specificity of the HA antibody, examination of HFF monolayers infected with the parental strain PRUΔ*hxgprt* did not yield any HA staining by IFA (data not shown). In vacuoles of 2- and 4-dpi bradyzoites expressing BPK1-HA, this protein could be detected outside the parasite in the lumen of the cyst (Fig. 3B and C). Similar results were observed for MCP4-HA in IFA analyses of HFF monolayers containing 2- and 4-dpi bradyzoites expressing MCP4-HA (Fig. 3E and F). Enrichment of both BPK1-HA and MCP4-HA is seen at the periphery of the vacuole in the area coincident with the cyst wall, as shown by colocalization with DBA staining (Fig. 3B, C, E, and F). While the secreted forms of both BPK1-HA and MCP4-HA could be visualized, neither protein could be detected within the intracellular parasites by these methods (data not shown). Examination of HFF monolayers infected with 2-dpi tachyzoites expressing BPK1-HA demonstrated that the fusion protein could be detected in some of the vacuoles; however, we observed that

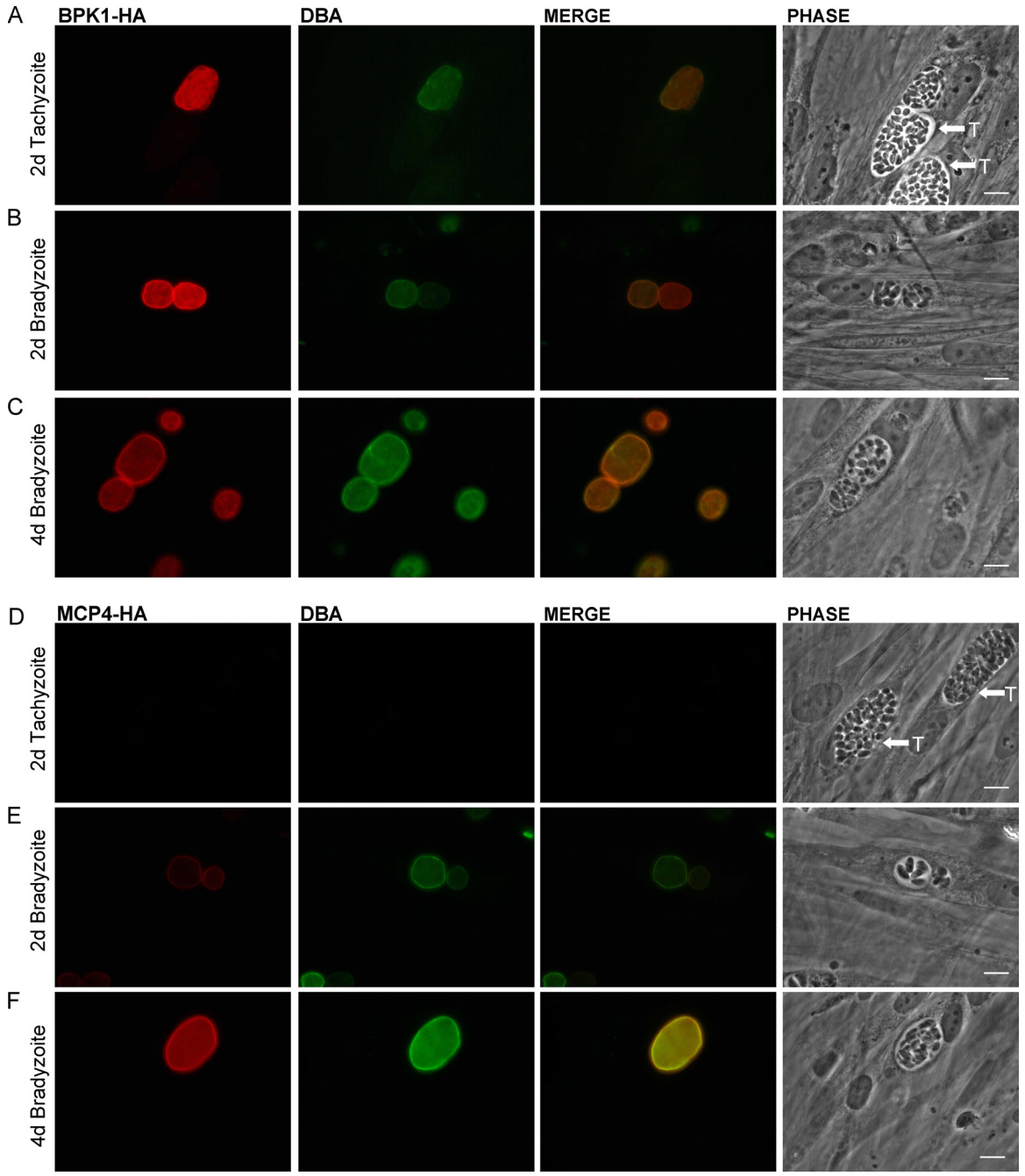

FIG. 3. BPK1 and MCP4 localize to the lumen and wall area of *in vitro* bradyzoite cysts. HFF monolayers on glass coverslips were infected with PRUΔ*hxgprt* parasites expressing BPK1-HA (A to C) or MCP4-HA (D to F) for 2 days (A, D) under tachyzoite growth conditions and for 2 days (B, E) or 4 days (C, F) under bradyzoite growth conditions. Coverslips were fixed and stained, as indicated, with rat anti-HA (red) and DBA (green) as described in Materials and Methods. The corresponding merged and phase images are also shown. A capital T indicates tachyzoite vacuoles. Representative images from at least two independent experiments are shown. Scale bars represent 10 μm.

BPK1-HA staining was always coincident with DBA staining, thus indicating cyst wall formation in these vacuoles (Fig. 3A). These results reflect the low levels of bradyzoite conversion events that occur under tachyzoite conditions. Examination of those monolayers infected with 2-dpi tachyzoites expressing MCP4-HA demonstrated that while DBA^+ vacuoles with secreted MCP4-HA staining in tachyzoite cultures were also observed (data not shown), these vacuoles were observed more infrequently than BPK1-HA^+ DBA^+ vacuoles, consistent with the relatively lower levels of MCP4-HA versus BPK1-HA protein (Fig. 2). Collectively, these results confirm that BPK1 and MCP4 are bradyzoite proteins secreted into the lumen of the cyst, where they localize to the cyst wall area. Due to our inability to detect these proteins within the parasite, however, we are unable at this time to determine the secretory organelle from which they originate.

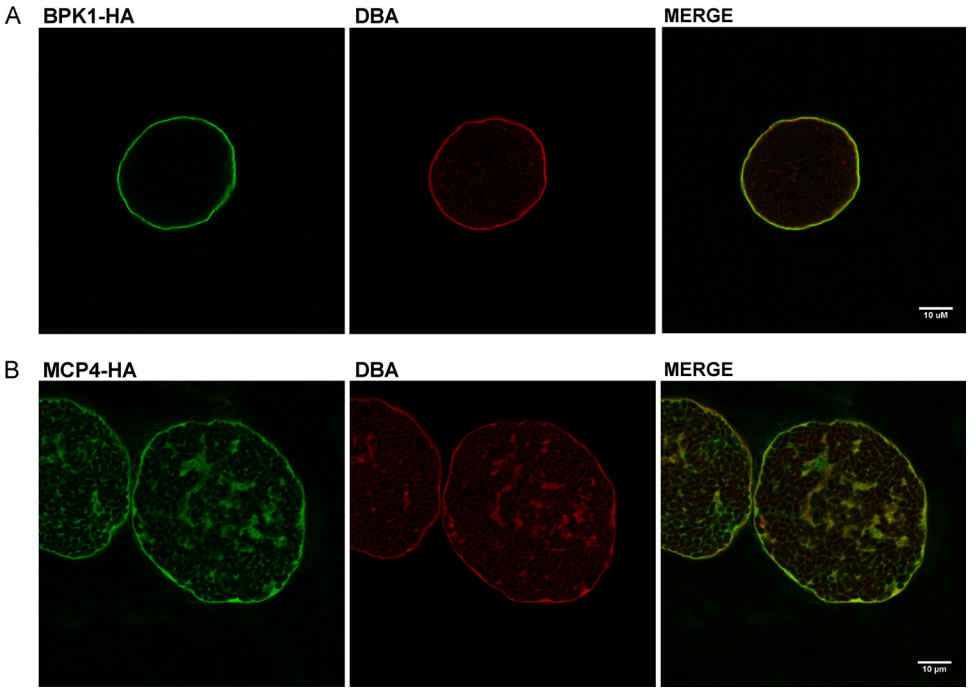

FIG. 4. BPK1 and MCP4 localize to the cyst periphery *in vivo*. Forty-micrometer coronal brain sections from mice infected 40 days previously with parasites expressing BPK1-HA (A) or MCP4-HA (B) were probed for HA (green) and DBA (red) and examined by confocal microscopy as described in Materials and Methods. The corresponding merged images are also shown. Scale bars represent 10 μm.

BPK1 and MCP4 localization *in vivo*. While these studies demonstrate that BPK1-HA and MCP4-HA are secreted into the cysts of *in vitro* bradyzoites, further studies were necessary to confirm that the secretion of these proteins is maintained in *in vivo* bradyzoite cysts. For example, another bradyzoite-secreted factor, BRP1, is differentially secreted by *in vitro* and *in vivo* bradyzoites (45). To determine BPK1-HA and MCP4-HA localization in *in vivo Toxoplasma* cysts, 40-dpi brain sections from mice infected with either of the parasites expressing the respective fusion proteins were probed with HA-specific antisera, as well as DBA for visualization of the cyst wall, and then examined by confocal microscopy. Consistent with the *in vitro* model of cyst formation, we observed BPK1-HA and MCP4-HA staining in the lumen of the cysts with intense staining at the periphery consistent with the cyst wall, as confirmed by colocalization with DBA staining (Fig. 4A and B, respectively). These results confirm that BPK1 and MCP4 are bradyzoite-secreted proteins that localize to the lumen and wall region of the cyst in both *in vitro* and *in vivo* bradyzoites.

BPK1 and MCP4 are components of the cyst wall. BPK1 and MCP4 are seen at the periphery and lumen of the tissue cyst; however, more precise methods are needed to show localization to the cyst wall. To identify if these proteins are components of the cyst wall, EM was used to determine the localization of BPK1-HA and MCP4-HA in *in vitro* or *in vivo* cysts. BPK1-HA was found to be a wall component of 5-dpi *in vitro* cysts, as shown by the presence of numerous gold particles in the cyst wall (Fig. 5A and B). Gold particles corresponding to MCP4-HA also localized within the cyst wall in 40-dpi *in vivo*-derived cysts (Fig. 5C). No specific localization of either BPK1 or MCP4, however, was observed within the bradyzoite parasites. Together, these results demonstrate that BPK1 and MCP4 are bradyzoite-secreted components of the *Toxoplasma* cyst wall.

DISCUSSION

We have characterized the transcriptome of the *Toxoplasma* asexual developmental stages, tachyzoites and bradyzoites, using both *in vitro*- and *in vivo*-derived bradyzoites. *In vivo* bradyzoites were isolated at 21 dpi, at which time tissue cysts have formed and tachyzoites are no longer detected (20). Sulfadiazine treatment, which inhibits parasite dihydropteroate synthase (DHPS), was necessary to allow the animals to survive the high infectious dose of *Toxoplasma*. This treatment is often used to allow the development of persistent infection in animals which would not otherwise survive the acute infection (17). It is important, therefore, to note when interpreting the data that the comparison between 4-dpi *in vitro* bradyzoites and 21-dpi *in vivo* bradyzoites is also a comparison of parasites with and without sulfadiazine, as well as growth within different cell types and species (human fibroblast cells versus mouse brain tissue). How these variables might impact the comparisons is not known, but the data shown here on known developmentally regulated genes (Table 2) are all consistent with previous reports on their expression levels in the two stages (29, 31, 45). *In vitro* bradyzoites from 4 and 8 days of culture were examined in these expression arrays. The 8-day bradyzoites were not found to be any more similar to the 21-day *in vivo* bradyzoites than the 4-day bradyzoites were to the *in vivo* parasites (Fig. 1A and data not shown). This indicates that, at least at the transcript level, a longer time of *in vitro* bradyzoite

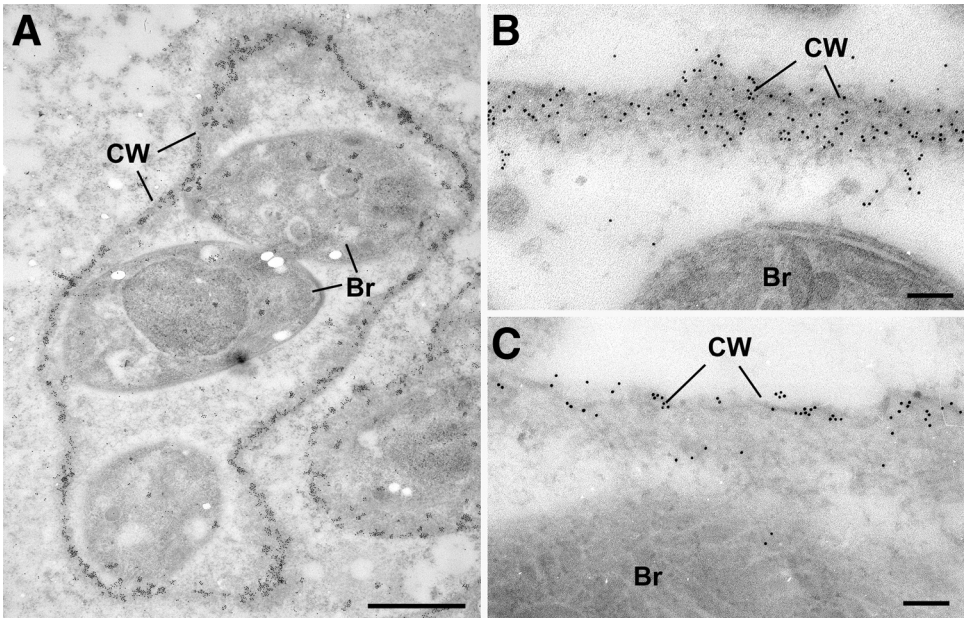

FIG. 5. BPK1 and MCP4 localize to the cyst wall. EM of tissue cysts stained for BPK1-HA (A and B) and for MCP4-HA (C) using an anti-HA antibody and visualized with 10-nm gold particles. (A) Low-power magnification of a small *in vitro* tissue cyst (5 dpi) containing bradyzoites (Br) showing numerous gold particles over the cyst wall (CW). Bar represents 1 μm. (B) Detail of the periphery of a 5-day *in vitro* tissue cyst labeled for BPK1 illustrating the numerous gold particles associated with the cyst wall. Bar represents 100 nm. (C) Detail of the periphery of an *in vivo*-derived tissue cyst (40 dpi) labeled with MCP4 showing the gold particles specifically associated with the cyst wall. Bar represents 100 nm.

growth does not make the *in vitro* bradyzoites more closely resemble *in vivo* bradyzoites.

The populations of bradyzoites used in this study were likely in different stages of the cell cycle; *in vivo* bradyzoites are believed to be dividing at a much lower rate than tachyzoites, and so a greater fraction of the former are likely in the G_1 or G_0 (arrested) stage of the cell cycle, whereas parasites transitioning from the tachyzoite to the bradyzoite stage *in vitro* have many cells in late S/G_2, a difference that may be key to the differentiation process (21, 39, 48). Work by Behnke et al. has demonstrated distinct subtranscriptomes in tachyzoites as they progress through the cell cycle (5). While there are no such cell cycle data for bradyzoites, it seems likely that differences between *in vitro* (4d Brady) and *in vivo* (21d Brady) bradyzoites will include a mixture of cell cycle- and development-related changes. Consistent with this, transcript levels for motor/dynein and cytoskeleton-related genes, which are most highly expressed by synchronous tachyzoites during the S/M stage of the tachyzoite cell cycle (5), were found to be higher in the 4d Brady samples than in the 21d Brady samples. Such differences between 4d Brady and 21d Brady samples, however, were not seen for transcript levels of microneme- and rhoptry-secreted proteins, which are also most highly expressed in the S/M stage, suggesting that, at least for these families, developmental regulation supersedes cell cycle regulation (see Table S3A and B in the supplemental material).

Genes whose proteins localize to the secretory organelles of *Toxoplasma* are of particular interest because of their role in invasion, host cell modulation, and modification of the PV. Transcript levels corresponding to several invasion-associated microneme proteins were significantly changed in bradyzoites versus tachyzoites, including two microneme-localized proteins, MIC12 and MIC13, which were upregulated in bradyzoites (see Table S3A in the supplemental material). MIC13 is a MAR domain-containing micronemal protein that has been shown to preferentially bind to certain sialyloligosaccharide probes versus MIC1, including to a sugar which is enriched in the mouse gut (22). As bradyzoites must invade after oral infection, this upregulation of MIC13 suggests that *Toxoplasma* expresses a different repertoire of proteins to tailor its invasion machinery to the different host environments that a given life cycle stage will encounter.

Transcript data for 15 known rhoptry proteins showed significant developmental regulation between tachyzoites and bradyzoites (Fig. 2B). Most of these are downregulated by bradyzoites, including the active kinase ROP16, which modulates STAT activity and interleukin-12 secretion (44). The probe set for ROP5 transcripts, another key protein in the host-parasite interaction (4, 41), had a decreased signal as well; note, however, that the multiple, tandem copies of ROP5 (4, 41) are not distinguishable on this array, and so additional analyses are needed to determine whether there are differences in how the various ROP5 isoforms are expressed during the tachyzoite-to-bradyzoite transition. As previously reported (32), ROP8, another predicted pseudokinase and member of the ROP2 family, was upregulated in the bradyzoite samples versus tachyzoites, perhaps to substitute for or augment the function of ROP2 family members with decreased expression, such as ROP11 and, possibly, ROP5. Regardless, the developmental regulation of rhoptry-secreted effectors argues that bradyzoites likely differ in how they modify the PV and modulate host cell functions.

Dense-granule proteins (GRAs) are thought to be important for proper function of the PV, but for the most part, their roles

are unknown (33). Transcript levels corresponding to 6 of the previously identified GRAs are decreased in transcript abundance in bradyzoites, including NTPase I, whose tachyzoite-specific expression had previously been noted (20). Similarly, GRA4, -6, and -8 expression has previously been reported to be reduced or even not detectable within the bradyzoite PV (20). GRA7 showed a unique, transient expression profile in this data set whereby its expression was decreased in *in vitro* bradyzoites (4d Brady) versus that in tachyzoites (2d Tachy), but its expression returned to near tachyzoite levels in 21d Brady *in vivo* samples (see Table S3C in the supplemental material). Previous studies have shown that in *in vivo* bradyzoite cysts, GRA7 is reduced in the PV but strong staining is detected in the dense granules (20). Together with our array data, this suggests that GRA7 may not be vital to maintaining the cyst vacuole but is available in the dense granules for secretion when a new PV is established. Only one dense-granule-secreted protein, GRA9, had significantly increased transcript levels in bradyzoites (see Table S3C in the supplemental material) (1). What role GRA9 might play in the tissue cyst is completely unknown.

Among the proteins that were upregulated in bradyzoites and predicted to be secreted, BPK1 and MCP4 were chosen for further investigation. These were found to localize to the cyst wall and lumen *in vitro* and *in vivo*, thus supporting the utility of this method in identifying bradyzoite-secreted effectors. The presence of a protein with sugar-binding MAR domains that localizes to the glycoconjugate-rich cyst wall suggests that MCP4 could be associating with the cyst wall by binding to carbohydrate moieties. As to the identities of such sugars, MCP4 is missing threonine residues conserved in the MIC1 MAR domain binding pocket which interact with sialic acid residues (8, 22), suggesting that this sugar, at least, is not a crucial part of its ligand-binding repertoire.

The accuracy of signal peptide prediction depends upon the reliability of the gene predictions and the choice of ATG start codon, which are two of the most difficult challenges for gene prediction software. Hence, the list of predicted, bradyzoite-secreted candidates described here is likely an imperfect inventory but it does serve as a valuable list of candidates for further analysis. Many on this list have no homology to proteins with known functions, but several do, including 4 putatively secreted effectors with kinase domains. Kinases and inactive pseudokinases are proving to be crucial to *Toxoplasma* infection (19, 41, 44), so these bradyzoite-upregulated kinases are likely to be important, whether they are secreted into the host cell or into the cyst lumen. Also identified in this data set were proteins that may be important to the bradyzoite cyst structure. These include proteins homologous to previously identified oocyst wall components that are thought to be highly cross-linked (6). Similarly, many upregulated transcripts encoded PAN domains that could also play a role in tissue cyst formation, although *Toxoplasma* proteins with PAN domains have been described primarily as invasion-associated proteins (12). PAN domains contain disulfide bonds and are thought to mediate a broad range of protein-protein and protein-carbohydrate interactions (47). One bradyzoite-upregulated transcript encoding a protein with a PAN domain (TGME49_032400/44.m04666) was show by Chen et al. to be secreted into the PV when ectopically expressed by tachyzoites (12), suggesting that it might play a role in the cyst structure. Overall, the work described here presents the first genome-wide analysis of changes in the transcriptome associated with bradyzoite development *in vitro* and *in vivo*. The utility of this data set has been demonstrated by the identification and characterization of two novel bradyzoite-specific proteins that appear to play a role in the tissue cyst wall. Further analyses of these data sets will likely reveal important changes in metabolism and other ways in which this crucial developmental form performs its key role in the transmission of *T. gondii*.

ACKNOWLEDGMENTS

We acknowledge the Stanford Protein and Nucleic Acid Facility and Cell Science Imaging Facility at Stanford University.

This work was supported in part by the NIH (AI 41014) and a subcontract from EuPathDB.org. K.R.B. was supported by NIH training grant T32 AI7328 and a postdoctoral fellowship (119025-PF-10-165-01-MPC) from the American Cancer Society. H.M.F. was supported by NIH T32 RR07038 and a KO1 award (KO1RR031487) from the National Center for Research Resources. D.J.F. was supported by an equipment grant from the Wellcome Trust.

REFERENCES

1. **Adjogble, K. D., et al.** 2004. GRA9, a new Toxoplasma gondii dense granule protein associated with the intravacuolar network of tubular membranes. Int. J. Parasitol. **34:**1255–1264.
2. **Asai, T., and S. Tomavo.** 2007. Biochemistry and metabolism of *Toxoplasma gondii*, p. 185–206. *In* L. M. Weiss and K. Kim (ed.), *Toxoplasma gondii*: the model apicomplexan. Perspectives and methods. Academic Press, London, United Kingdom.
3. **Bahl, A., et al.** 2010. A novel multifunctional oligonucleotide microarray for Toxoplasma gondii. BMC Genomics **11:**603.
4. **Behnke, M. S., et al.** 2011. Virulence differences in Toxoplasma mediated by amplification of a family of polymorphic pseudokinases. Proc. Natl. Acad. Sci. U. S. A. **108:**9631–9636.
5. **Behnke, M. S., et al.** 2010. Coordinated progression through two subtranscriptomes underlies the tachyzoite cycle of Toxoplasma gondii. PLoS One **5:**e12354.
6. **Belli, S. I., N. C. Smith, and D. J. Ferguson.** 2006. The coccidian oocyst: a tough nut to crack! Trends Parasitol. **22:**416–423.
7. **Bendtsen, J. D., H. Nielsen, G. von Heijne, and S. Brunak.** 2004. Improved prediction of signal peptides: SignalP 3.0. J. Mol. Biol. **340:**783–795.
8. **Blumenschein, T. M., et al.** 2007. Atomic resolution insight into host cell recognition by Toxoplasma gondii. EMBO J. **26:**2808–2820.
9. **Boothroyd, J. C., and J. F. Dubremetz.** 2008. Kiss and spit: the dual roles of Toxoplasma rhoptries. Nat. Rev. Microbiol. **6:**79–88.
10. **Carruthers, V., and J. C. Boothroyd.** 2007. Pulling together: an integrated model of Toxoplasma cell invasion. Curr. Opin. Microbiol. **10:**83–89.
11. **Cérède, O., et al.** 2005. Synergistic role of micronemal proteins in Toxoplasma gondii virulence. J. Exp. Med. **201:**453–463.
12. **Chen, Z., O. S. Harb, and D. S. Roos.** 2008. In silico identification of specialized secretory-organelle proteins in apicomplexan parasites and in vivo validation in Toxoplasma gondii. PLoS One **3:**e3611.
13. **Cleary, M. D., U. Singh, I. J. Blader, J. L. Brewer, and J. C. Boothroyd.** 2002. Toxoplasma gondii asexual development: identification of developmentally regulated genes and distinct patterns of gene expression. Eukaryot. Cell **1:**329–340.
14. **Coppin, A., et al.** 2003. Developmentally regulated biosynthesis of carbohydrate and storage polysaccharide during differentiation and tissue cyst formation in Toxoplasma gondii. Biochimie **85:**353–361.
15. **Craver, M. P., P. J. Rooney, and L. J. Knoll.** 2010. Isolation of Toxoplasma gondii development mutants identifies a potential proteophosphogylcan that enhances cyst wall formation. Mol. Biochem. Parasitol. **169:**120–123.
16. **Donald, R. G., D. Carter, B. Ullman, and D. S. Roos.** 1996. Insertional tagging, cloning, and expression of the Toxoplasma gondii hypoxanthine-xanthine-guanine phosphoribosyltransferase gene. Use as a selectable marker for stable transformation. J. Biol. Chem. **271:**14010–14019.
17. **Dubey, J. P., D. S. Lindsay, and C. A. Speer.** 1998. Structures of *Toxoplasma gondii* tachyzoites, bradyzoites, and sporozoites and biology and development of tissue cysts. Clin. Microbiol. Rev. **11:**267–299.
18. **Durbin, B. P., J. S. Hardin, D. M. Hawkins, and D. M. Rocke.** 2002. A variance-stabilizing transformation for gene-expression microarray data. Bioinformatics **18**(Suppl. 1)**:**S105–S110.
19. **El Hajj, H., et al.** 2007. ROP18 is a rhoptry kinase controlling the intracellular proliferation of Toxoplasma gondii. PLoS Pathog. **3:**e14.

20. **Ferguson, D. J.** 2004. Use of molecular and ultrastructural markers to evaluate stage conversion of Toxoplasma gondii in both the intermediate and definitive host. Int. J. Parasitol. **34:**347–360.
21. **Ferguson, D. J., and W. M. Hutchison.** 1987. An ultrastructural study of the early development and tissue cyst formation of Toxoplasma gondii in the brains of mice. Parasitol. Res. **73:**483–491.
22. **Friedrich, N., et al.** 2010. Members of a novel protein family containing microneme adhesive repeat domains act as sialic acid-binding lectins during host cell invasion by apicomplexan parasites. J. Biol. Chem. **285:**2064–2076.

22a. **Fritz, H., B. Barr, A. Packham, A. Melli, and P. A. Conrad.** 20 October 2011. Methods to produce and safely work with large numbers of *Toxoplasma gondii* oocysts and bradyzoite cysts. J. Microbiol. Methods. doi:10.1016/j.mimet.2011.10.010.

23. **Fux, B., et al.** 2007. Toxoplasma gondii strains defective in oral transmission are also defective in developmental stage differentiation. Infect. Immun. **75:**2580–2590.
24. **Gautier, L., L. Cope, B. M. Bolstad, and R. A. Irizarry.** 2004. affy—analysis of Affymetrix GeneChip data at the probe level. Bioinformatics **20:**307–315.
25. **Gutierrez, J., et al.** 2010. Detection and quantification of Toxoplasma gondii in ovine maternal and foetal tissues from experimentally infected pregnant ewes using real-time PCR. Vet. Parasitol. **172:**8–15.
26. **Hanks, S. K., and T. Hunter.** 1995. Protein kinases 6. The eukaryotic protein kinase superfamily: kinase (catalytic) domain structure and classification. FASEB J. **9:**576–596.
27. **Huber, W., A. von Heydebreck, H. Sultmann, A. Poustka, and M. Vingron.** 2002. Variance stabilization applied to microarray data calibration and to the quantification of differential expression. Bioinformatics **18**(Suppl. 1)**:**S96–S104.
28. **Huskinson-Mark, J., F. G. Araujo, and J. S. Remington.** 1991. Evaluation of the effect of drugs on the cyst form of Toxoplasma gondii. J. Infect. Dis. **164:**170–171.
29. **Kim, S. K., A. Karasov, and J. C. Boothroyd.** 2007. Bradyzoite-specific surface antigen SRS9 plays a role in maintaining *Toxoplasma gondii* persistence in the brain and in host control of parasite replication in the intestine. Infect. Immun. **75:**1626–1634.
30. **Lescault, P. J., et al.** 2010. Genomic data reveal Toxoplasma gondii differentiation mutants are also impaired with respect to switching into a novel extracellular tachyzoite state. PLoS One **5:**e14463.
31. **Lyons, R. E., R. McLeod, and C. W. Roberts.** 2002. Toxoplasma gondii tachyzoite-bradyzoite interconversion. Trends Parasitol. **18:**198–201.
32. **Manger, I. D., et al.** 1998. Expressed sequence tag analysis of the bradyzoite stage of *Toxoplasma gondii*: identification of developmentally regulated genes. Infect. Immun. **66:**1632–1637.
33. **Mercier, C., K. Adjogble, W. Daubener, and M. Delauw.** 2005. Dense granules: are they key organelles to help understand the parasitophorous vacuole of all apicomplexa parasites? Int. J. Parasitol. **35:**829–849.
34. **Montoya, J., J. Kovacs, and J. Remington.** 2005. *Toxoplasma gondii*, p. 3170–3197. *In* G. Mandell, J. Bennett, and R. Dolin (ed.), Principles and practice of infectious diseases, 6th ed. Elsevier, Philadelphia, PA.
35. **Nielsen, H., J. Engelbrecht, S. Brunak, and G. von Heijne.** 1997. Identification of prokaryotic and eukaryotic signal peptides and prediction of their cleavage sites. Protein Eng. **10:**1–6.
36. **Nielsen, H., and A. Krogh.** 1998. Prediction of signal peptides and signal anchors by a hidden Markov model. Proc. Int. Conf. Intell. Syst. Mol. Biol. **6:**122–130.
37. **Ong, Y. C., M. L. Reese, and J. C. Boothroyd.** 2010. Toxoplasma rhoptry protein 16 (ROP16) subverts host function by direct tyrosine phosphorylation of STAT6. J. Biol. Chem. **285:**28731–28740.
38. **Peixoto, L., et al.** 2010. Integrative genomic approaches highlight a family of parasite-specific kinases that regulate host responses. Cell Host Microbe **8:**208–218.
39. **Radke, J. R., M. N. Guerini, M. Jerome, and M. W. White.** 2003. A change in the premitotic period of the cell cycle is associated with bradyzoite differentiation in Toxoplasma gondii. Mol. Biochem. Parasitol. **131:**119–127.
40. **R Development Core Team.** 2009. R: a language and environment for statistical computing. R Foundation for Statistical Computing, Vienna, Austria. http://www.R-project.org/.
41. **Reese, M. L., G. M. Zeiner, J. P. Saeij, J. C. Boothroyd, and J. P. Boyle.** 2011. Polymorphic family of injected pseudokinases is paramount in Toxoplasma virulence. Proc. Natl. Acad. Sci. U. S. A. **108:**9625–9630.
42. **Rocke, D., G. C. Lee, J. Tillinghast, B. Durbin-Johnson, and S. Wu.** 2010. LMGene: LMGene software for data transformation and identification of differentially expressed genes in gene expression arrays. Fred Hutchinson Cancer Research Center, Seattle, WA. http://www.bioconductor.org/packages/release/bioc/html/LMGene.html.
43. **Saeij, J. P., G. Arrizabalaga, and J. C. Boothroyd.** 2008. A cluster of four surface antigen genes specifically expressed in bradyzoites, SAG2CDXY, plays an important role in *Toxoplasma gondii* persistence. Infect. Immun. **76:**2402–2410.
44. **Saeij, J. P., et al.** 2007. Toxoplasma co-opts host gene expression by injection of a polymorphic kinase homologue. Nature **445:**324–327.
45. **Schwarz, J. A., A. E. Fouts, C. A. Cummings, D. J. Ferguson, and J. C. Boothroyd.** 2005. A novel rhoptry protein in Toxoplasma gondii bradyzoites and merozoites. Mol. Biochem. Parasitol. **144:**159–166.
46. **Soldati, D., and J. C. Boothroyd.** 1993. Transient transfection and expression in the obligate intracellular parasite Toxoplasma gondii. Science **260:**349–352.
47. **Tordai, H., L. Banyai, and L. Patthy.** 1999. The PAN module: the N-terminal domains of plasminogen and hepatocyte growth factor are homologous with the apple domains of the prekallikrein family and with a novel domain found in numerous nematode proteins. FEBS Lett. **461:**63–67.
48. **Weiss, L. M., and K. Kim.** 2007. Bradyzoite development, p. 341–366. *In* L. M. Weiss and K. Kim (ed.), *Toxoplasma gondii*: the model apicomplexan. Perspectives and methods. Academic Press, London, United Kingdom.
49. **Zhang, Y. W., S. K. Halonen, Y. F. Ma, M. Wittner, and L. M. Weiss.** 2001. Initial characterization of CST1, a *Toxoplasma gondii* cyst wall glycoprotein. Infect. Immun. **69:**501–507.